Focus Article

Thermally responsive polymer–nanoparticle composites for biomedical applications

Laura E. Strong and Jennifer L. West*

Thermally responsive polymer–metal nanoparticle composites couple the ability of certain metal nanoparticles to convert external stimuli to heat with polymers that display sharp property changes in response to temperature changes, allowing for external control over polymer properties. These systems have been investigated for a variety of biomedical applications, including drug delivery, microfluidic valve control, and cancer therapy. This article focuses on three different size scales of this system: bulk systems (>1 mm), nano- or microscale systems, and individual particle coatings. These composite systems will continue to be widely researched in the future for their vast potential in various biomedical applications. *WIREs Nanomed Nanobiotechnol* 2011 3 307–317 DOI: 10.1002/wnan.138

INTRODUCTION

Thermally responsive polymers, materials that undergo phase changes that result in dramatic changes in material properties, have been under investigation for applications such as drug delivery for many decades.[1–3] A confounding issue to the translation of thermally responsive polymers in biomedical applications has been the need for mechanisms to locally change the temperature of the polymer material without damage to surrounding tissue. Recent advances in nanotechnology have provided nanoparticles that can induce localized heating upon exposure to light or alternating magnetic fields (AMFs). By creating composites of thermally responsive polymers with appropriate nanoparticles, it has been possible to generate materials where polymer phase changes can be induced by exposing the composite material to light or magnetic field, and this advance has enabled applications including pulsatile drug delivery and valves for microfluidic devices.

METAL NANOPARTICLES

Nanoparticles have been highly investigated for use in biological and medical applications due to their unique size and optical properties. The five main nanoparticle types that will be discussed in this article are solid gold nanoparticles (AuNPs), gold–gold sulfide (Au–Au_2S) nanoparticles, gold–silica (SiO_2–Au) nanoshells, gold nanorods, and superparamagnetic iron oxide (Fe_3O_4) nanoparticles. All these particles are utilized because of their ability to induce localized heating upon exposure to light (gold-based nanoparticles) or AMF (iron oxide nanoparticles). Additional properties of these particles are summarized in Table 1.

Heat Generation by Nanoparticles

When a gold-based nanoparticle is irradiated with light at the wavelength of its surface plasmon resonance, this light is rapidly transferred into thermal energy, causing a localized temperature increase.[4,5,10] Au–Au_2S nanoparticles, silica–Au nanoshells, and Au nanorods can all be tuned to have a surface plasmon resonance in the near-infrared (NIR) range.[5–7,10] The NIR range (700–900 nm) is above the absorption of biological molecules such as hemoglobin (<650 nm) and below the range absorbed by water (>900 nm).[11] Thus, NIR light is of particular interest for biological applications, as these wavelengths penetrate biological tissue with relatively little attenuation or tissue damage, as demonstrated in Figure 1. Alternatively, superparamagnetic Fe_3O_4 nanoparticles generate heat when exposed to an AMF.[8] This heat is generated due to magnetic hysteresis loss, and the amount of heat generated is dependent on the magnetic properties of the nanoparticles as well as the strength and frequency

*Correspondence to: jwest@rice.edu
Department of Bioengineering, Rice University, Houston, TX, USA
DOI: 10.1002/wnan.138

TABLE 1 | Nanoshell Properties[4–9]

Au Nanoparticles	Au–Au_2S Nanoparticles	Silica–Au Nanoshells	Au Nanorods	Iron Oxide Nanoparticles
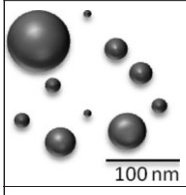	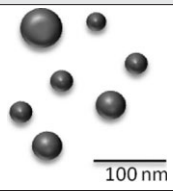	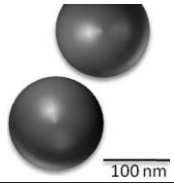	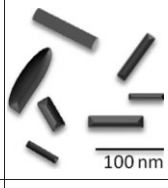	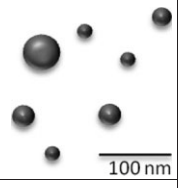
Diameter: 2–100 nm	Diameter: 30–40 nm	Diameter: 120–150 nm	Aspect Ratio:1.5–10 (ex: 20×100 nm)	Diameter: <100 nm
Extinction: 520–575 nm	Extinction (tunable): ~850 nm	Extinction (tunable): ~800 nm	Extinction: 600–1300 nm	Extinction: n/a
Pros: highly investigated, ease of synthesis	Pros: NIR absorbance	Pros: NIR absorbance	Pros: NIR absorbance	Pros: Heat generation by AMF exposure
Cons: extinction coefficent near that of hemoglobin	Cons: synthesis byproduct of gold colloid	Cons: large	Cons: surfactant toxicity from synthesis	Cons: Large dose required *in vivo*

AMF, alternating magnetic field; NIR, near-infrared.

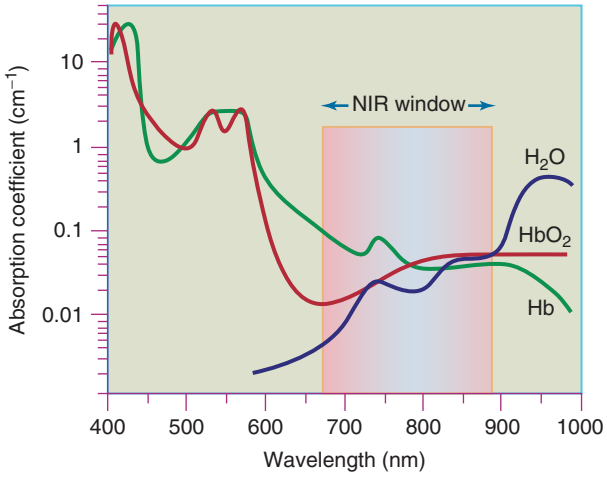

FIGURE 1 | Near-infrared light (650–900 nm) is of particular interest in biological applications as it is minimally absorbed by biological chromophores and water. (Reprinted with permission from Ref 11. Copyright 2001 Macmillan Publishers Ltd)

of oscillation of the AMF.[8] The applied magnetic fields do not affect healthy tissue.[8]

Solid Gold Nanoparticles

Gold nanoparticles (AuNPs, also called gold colloids) are one of the most stable and highly investigated metal nanoparticles.[4] These particles, thought of as 'soluble gold' in antiquity, were used for esthetic and curative purposes as early as the fourth and fifth century BC.[4] Several synthesis techniques exist, the most common being citrate reduction of chloroauric acid ($HAuCl_4$) in water.[12] These particles (with diameters ranging from 2 to 100 nm) have maximum absorption around 520–575 nm, depending on the diameter of the particles, with the smaller particles maximally absorbing at a lower wavelength.[4]

Gold–Gold Sulfide Nanoparticles

Gold–gold sulfide (Au–Au_2S) nanoparticles were first developed by Zhou et al.[13] Due to their optical properties, these particles were originally thought to consist of a dielectric gold–silica core surrounded by a thin gold shell.[5] Controversy still remains over the exact structure of these particles; however, the core/shell model fits the optical data and surface conjugation studies also suggest a continuous gold coating.[14] These nanoparticles are synthesized by mixing $HAuCl_4$ and sodium sulfide (Na_2S).[13] The ratios of these two materials can be adjusted to alter surface plasmon resonance of the particles from 600 nm to greater than 1000 nm.[15] Much research has been done on Au–Au_2S nanoparticles that are NIR absorbing; these particles generally have a 35–55 nm diameter and a surface plasmon resonance near 800–900 nm.[5,16–20]

Gold–Silica Nanoshells

Gold–silica nanoshells were developed by Oldenburg et al. through molecular self-assembly and colloid reduction chemistry.[21] These particles consist of a dielectric silica core surrounded by a solid gold shell, and adjustments of these two parameters provide optimal control over the optical properties of the particles, as seen in Figure 2. The peak extinction

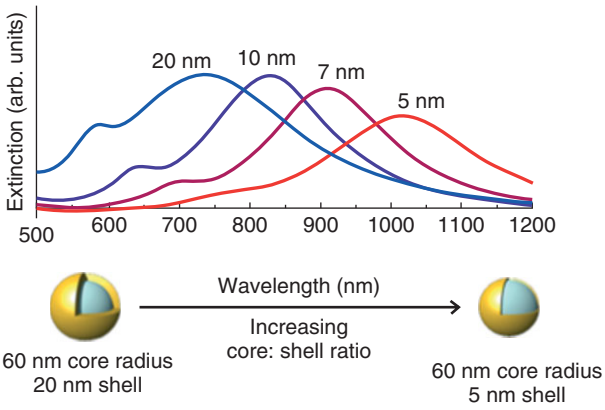

FIGURE 2 | By altering gold–silica nanoshell core:shell ratios, optical tunability can be obtained. A thinner shell causes a red shift in absorbance. (Reprinted with permission from Ref 6. Copyright 2006 Spring Science + Business Media)

coefficients of these particles can range from visible to NIR and even infrared ranges.[6] Most photothermal studies have utilized particles with a 120 nm core and 10 nm shell, as this corresponds to a peak absorption coefficient in the NIR range, where biological tissue is most permissive of light.[6,18,22–26]

To synthesize these particles, silica cores are created using the Stöber method and then surface functionalized with amine groups using silane reagents. Small gold-colloid particles (~2 nm) are then absorbed onto the aminated surface to form gold nucleation sites.[6] A final reduction step in chloroauric acid, potassium carbonate, and formaldehyde produces a gold shell between 5 and 30 nm thickness.[6]

Gold Nanorods

Gold nanorods are anisotropic nanoparticles composed of solid gold, where particle shape strongly influences optical properties. Gold nanorods show a surface plasmon band near 520 nm similar to spherical AuNPs, but also have a second band at a longer wavelength.[27] These optical properties are much more dependent on the particle's aspect ratio (ratio of length to diameter).[7] The dominant surface plasmon band occurs at a longer wavelength and is based on the axial length of the particle.[7] The secondary surface plasmon band occurs around 520 nm due to the weaker transverse resonance.[7] Particles with larger aspect ratios will have the primary longitudinal resonance at a longer wavelength than particles with a smaller aspect ratio.[7] These particles can be synthesized either by use of rigid templates or, more commonly, by use of seed and growth solutions in the presence of surfactants.[28]

Superparamagentic Iron Oxide Nanoparticles

Iron oxide nanoparticles, also called magnetite, have been investigated for use in several applications, including drug delivery, magnetic resonance imaging (MRI), hyperthermia, and tissue repair.[8] These particles are generally less than 100 nm in diameter and must be synthesized with a narrow particle size distribution and biocompatible surface coating.[8] Several synthesis mechanisms exist, with wet chemical methods shown to provide tighter control over the size and composition of the particles.[8] Exposure of these particles to an AMF results in localized heating.[8]

THERMALLY RESPONSIVE POLYMERS

Stimuli-responsive 'smart' polymers undergo fast, reversible conformational changes in response to small changes in the environment.[29] These changes usually involve the polymer microstructure transitioning between a hydrophilic and a hydrophobic state, altering chain conformation such that macroscopic material size and properties change as well.[29] Systems responsive to local chemical changes, such as changes in pH, as well as systems responsive to external stimuli, such as ultrasound, light, or temperature, have been studied.[30] Temperature-sensitive systems are easy to synthesize and control, making them suitable for many applications.[30] Commonly studied temperature-sensitive polymers include acrylamide-based hydrogels, especially poly[*N*-isopropylacrylamide] (PNIPAAm), as well as elastin-like polypeptides (ELPs).[3,29–31]

At a temperature-sensitive polymer's lower critical solution temperature (LCST), a reversible volume phase transition occurs. At lower temperatures, it is thermodynamically favorable for water molecules to form hydrogen bonds with polar groups on the polymer chains, causing the hydrogel to be in its swollen state. At higher temperatures, the increase in Gibbs free energy (ΔG) causes hydrogen bonding between the water molecules and polymer chains to become thermodynamically unfavorable compared to polymer–polymer and water–water interactions.[32] This causes the water to move into bulk solution and the polymer chains to collapse onto themselves forming hydrophobic interactions.[33] A common property characterized in thermally responsive systems is the polymer's deswelling ratio, a measurement of the degree of collapse a hydrogel undergoes at its LCST.

N-isopropylacrylamide

PNIPAAm is a widely studied thermally responsive polymer that exhibits an LCST near physiological

temperatures.[30] Pure PNIPAAm hydrogels have an LCST range of 25–32°C, and by incorporating a more hydrophilic comonomer into the hydrogel, this LCST can be raised to near 45–50°C.[34] Common comonomers used include acrylamide (AAm) or acrylic acid (AAc), with a 95:5 molar ratio of NIPAAm:AAm resulting in a gel with an LCST of approximately 40°C.[19] In addition, incorporation of *N*-isopropylmethacrylamide (NIPMAAm) increases the LCST due to the phase transition being inhibited by the steric hindrance of the additional methyl group.[35] In contrast, hydrogels consisting of hydrophilic acrylamide/acrylic acid monomers exhibit a positive volume change with increasing temperatures.[36,37]

Elastin-like Polypeptides

ELPs are synthetic peptides derived from the sequence of the hydrophobic domain of tropoelastin.[38] ELPs generally consist of oligiomeric repeats of the pentapeptide VPGXG (where X is any amino acid except proline).[38] By using recombinant methods to create these polymers, a monodisperse product with little batch-to-batch variability can be achieved, which is highly advantageous over synthetic polymer materials.[3,30,31] By altering amino acid sequence or number of repeats, ELP LCSTs are highly tunable and can be brought to above physiological temperatures.[3,31]

BULK HYDROGEL SYSTEMS

Several systems have been developed that consist of bulk hydrogels (diameter >1 mm) with encapsulated nanoparticles for applications including drug delivery,[19,20,25,39] microfluidic[23,24,40] and microlens[41] control. Additionally, the effects of these encapsulated nanoparticles on polymer bulk properties have been investigated.[42,43]

Drug Delivery

Drug delivery applications have been investigated using both NIR-absorbing nanoparticles and iron oxide nanoparticles. By combining thermally responsive polymers with encapsulated nanoparticles, pulsatile drug release triggered by an external stimulus can be achieved. A schematic of this process is shown in Figure 3.

Photothermally modulated drug delivery was first shown by Sershen et al. using a combination of *N*-isopropylacrylamide-co-acrylamide (NIPAAm-co-AAm) and gold–gold sulfide nanoparticles.[19] This study used hydrogels with a 95:5 molar ratio of

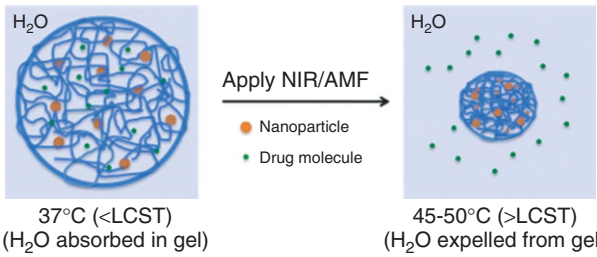

FIGURE 3 | Schematic of drug delivery from bulk hydrogels.

NIPAAm:AAm to achieve an LCST slightly above physiological temperature. Upon NIR irradiation of these composites, the temperature of the hydrogel exceeds the LCST, causing a burst release of any soluble molecules contained in the hydrogel matrix. Enhanced release of molecules such as methylene blue, ovalbumin, and bovine serum albumin was found to follow NIR irradiation of the nanoparticle-composite hydrogels.[19] Further investigation of this system showed that it could be applied to photothermal delivery of insulin.[20] A similar system using the same hydrogel formation with gold–silica nanoshells also successfully demonstrated photothermal drug delivery.[25] Studies showed that the collapse of hydrogel–nanoshell composites was controlled by both laser fluence and SiO_2 nanoshell concentration.[25] Photothermal release studies of methylene blue, insulin, and lysozyme showed a pulsatile drug release that was dependent on the molecular weight of the molecule.[25]

Drug delivery studies have also been investigated using iron oxide particles embedded in an NIPAAm-based matrix.[39,44–46] Bulk hydrogels were created using tetra(ethylene glycol) dimethacrylate (TEGDMA)[39,46] or poly(ethylene glycol) 400 dimethacrylate (PEG400DMA)[45] as a cross-linking agent. The incorporation of varying concentrations of iron oxide particles (20–30 nm diameter) showed no effect on swelling characteristics of the hydrogels.[44] These hydrogel discs were found to increase in temperature and collapse following exposure to an AMF.[39,45] A burst release of absorbed drugs, methylene blue, or vitamin B12 followed pulse application of AMF, with minimal diffusion of the drug out of the matrix without AMF.[39] This study showed these composites' potential as implanted, remotely controlled drug delivery devices.[39]

Microfluidic Valves

Due to remote triggering of dramatic changes in material size and shape, thermally responsive polymer–nanoparticle conjugates have been investigated

for use in the controlled manipulation of valves in microfabricated devices.

Sershen et al. proposed a combination of NIPAAm-co-AAm hydrogels, gold-colloid particles, and gold–silica particles for use in independent control of multiple valves within a microfluidic device, as seen in Figure 4.[23] Using these materials, independent control of two valves at a T-junction was achieved. One valve consisted of an NIPAAm-co-AAm gold-colloid nanoparticle composite, whereas the other contained NIPAAm-co-AAm gold–silica nanoshell composite. When exposed to green (532 nm) light, the gold-colloid channel opened and the gold–silica remained closed, but when exposed to NIR (832 nm) light, the gold–silica channel opened while the gold-colloid channel remained closed.[24] The authors noted that a larger number of independently controlled components could be achieved by using multiple nanoparticles with different absorption spectra, utilizing directed light, or tailoring the hydrogels to have differing LCSTs.[24] Additionally, Satarkar et al. have demonstrated microfluidic valve control using a NIPAAm–iron oxide nanocomposite combined with AMF.[40]

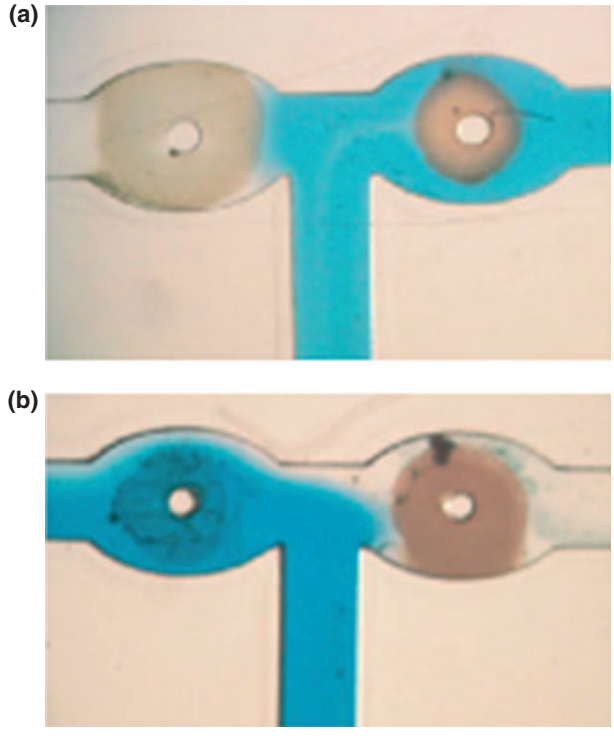

FIGURE 4 | T-junction in a microfluidic device formed by two valves: one made of a gold-colloid nanocomposite hydrogel and one made of a gold nanoshell composite hydrogel. (a) After the entire device is illuminated with 532 nm light for 5 seconds, the gold-colloid channel opened and the gold nanoshell channel remained closed. (b) The opposite response is seen when the device is illuminated with 832 nm light. (Reprinted with permission from Ref 24. Copyright 2005 Wiley-VCH Verlag GmbH & Co. KGaA)

Effects of Metal Nanoparticles on Bulk Hydrogel Properties

The Langer group has studied the effects of nanoparticle–polymer interactions on bulk hydrogel properties such as swelling, as well as methods to synthesize gold nanoparticles within a PNIPAAm matrix.[42,43] In this study, a PNIPAAm template was created using both *N*,*N*-methylene *bis*-acrylamide (MBAAm) and *N*,*N*-cystamine *bis*-acrylamide (CBAAm).[42,43] The CBAAm groups contain a disulfide bridge, which forms thiols and thiol-ethers capable of binding both Au^{3+} and AuNPs.[42,43] Once these hydrogels were formed, the gels were immersed in $KAuCl_4$ followed by $NaBH_4$ to allow for synthesis of AuNPs bound to thiol groups inside the PNIPAAm matrix.[42,43] The AuNP composite gels were found to have a higher degree of equilibrium swelling than PNIPAAm gels without AuNPs.[42,43] It is hypothesized that this is due to the Donnan effect of polyelectrolyte gels,[47] in which the surface charge of the AuNPs causes water afflux to balance the osmotic pressure build-up and the hydrogel to swell.[42,43] It was also noted that an increase in CBAAm concentration causes an increase in polymer hydrophilicity, resulting in the gel having an increased LCST.[42,43]

NANO/MICROSCALE COMPOSITES AND MICELLES

Although the majority of applications in this field focuses on either bulk (>1 mm) hydrogels or nanoscale coatings, a few groups have looked at micro-sized applications and micelles. Investigations have focused mostly on electrical and sensor properties of these materials[48–50] as well as their potential for drug delivery.[51,52] Micro- and nanoscale systems may potentially be amenable to targeted drug delivery applications as well.

Zhao et al. studied the electrical properties of microscale PNIPAAm hydrogels containing 5–10 nm AuNPs.[48,49] Vinyl groups were added to AuNPs by a reaction with allyl mercaptan.[49] These hydrogels were synthesized in the presence of AuNPs with attached vinyl groups, allowing the AuNPs to participate in the polymerization process as a cross-linker.[49] A significant deswelling was found to follow temperature increases from 18 to 32.5°C, with increasing AuNP concentration leading to a decrease in overall swelling because the particles are also acting as a cross-linker. As the hydrogel collapses, the distance between the

AuNPs decreases, resulting in an increase in electrical conductivity of the material.[49] The externally regulated thermo-switchability of these composites gives them many potential applications as sensors in nano and quantum electronics.[49]

A study by Li et al. investigated poly(styrene-b-*N*-isopropylacrylamide) micelles with surface-linked AuNPs (5 nm diameter).[50] DLS studies showed that the hydrodynamic diameter of these micelles decreased from 93 to 77 nm when the temperature was increased from 20 to 40°C. This system can also be tuned to have 10–35 AuNPs/micelle for use in sensor, catalyst, and electronic applications. Kim et al. have proposed combining hybrid AuNP/iron oxide nanoparticles with poly[*N*-isopropylacrylamide-co-acrylamide]-block-poly[ε-caprolactone] for combined hyperthermia and chemotherapy delivery with optical imaging.[51] This study used an 86:14 NIPAAm:AAm ratio to achieve an LCST of 42–45°C. Initial results show that the hydrodynamic diameter of these micelles decreases from 104 to 71 nm when temperature is increased from 25 to 45°C. Further optical and magnetic studies and characterization of this system are ongoing.[51]

The Peppas group has investigated the use of thermally responsive interpenetrating polymer networks (INPs) consisting of poly(AAm)/poly(AAc).[36,37] This system consisted of physically entangled polymer chains and exhibits a unique upper critical solution temperature, meaning the particles swell under elevated temperatures.[37] AuNPs (50 nm diameter) were encapsulated in a poly(AAm)/poly(AAc) INP.[36] The entire particle was found to have an average diameter of 300 nm and swelled up to 90 times its original volume when the temperature was increased from 25 to 40 ± 5°C.[36] In addition, the INP particles were PEGylated to prolong circulation time of the system *in vivo*.[36]

Hoare et al. developed a membrane-based drug delivery system consisting of an ethyl cellulose-iron oxide particle nanocomposite membrane with embedded PNIPAAm-based hydrogels, as shown in Figure 5. By applying an oscillating magnetic field to this device, the heat increase caused the nanogel to deswell, allowing a strong flux of drugs out of the reservoir. This device was synthesized by coevaporation to cause entrapment of PNIPPAm nanogels and iron oxide nanoparticles in the cellulose membrane.[52] The PNIPAAm gel was engineered to have an LCST above physiological temperature by incorporating NIPMAAm as well as AAm.[52] Analysis with sodium fluorescein showed approximately 20-fold increase in flux when the device was turned 'on' by exposure to an oscillating magnetic field, as well as consistent

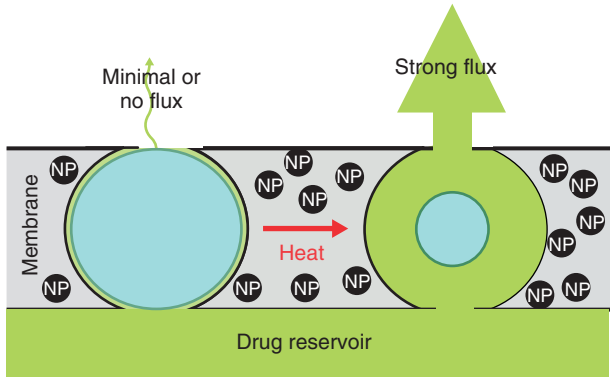

FIGURE 5 | Schematic of drug delivery from magnetically triggered nanogel composite membrane. (Reprinted with permission from Ref 52. Copyright 2009 American Chemical Society)

drug flux over four on–off cycles.[52] The authors note that the rapid swelling kinetics due to the size and engineered phase-transition behavior of the nanogels as well as the optimized size and surface chemistry of the iron oxide nanoparticles allow for rapid, repeatable, and tunable drug release under physiological conditions.[52]

POLYMER-COATED NANOPARTICLES

As of late, much focus has been placed on ways to apply a thermally responsive hydrogel coating on individual nanoparticles. This will allow particles to retain the same size properties as before, incorporated with the drug delivery potential of PNIPAAm-based systems discussed previously. Several synthesis methods have been investigated for this application including reversible addition fragmentation chain transfer (RAFT),[53–56] surfactant-free emulsion polymerization (SFEP),[26,57,58] surface-initiated atom transfer radical polymerization (SI-ATRP),[59–61] and other methods.[62,63] A summary of these techniques can be found in Table 2.

SFEP Methods

The work of Kim et al. investigates SFEP of poly(NIPAAm-co-AAc) onto AuNP and silica–Au nanoshells for drug delivery applications.[26,57,58] This synthesis method used a 94:6 wt% ratio of NIPAAm:AAc and *N*,*N*-methylenebisacrylamide (BIS) as a cross-linking agent. This process was carried out on 60 nm AuNP[57] and silica–Au nanoshells.[26] In addition, studies using an SFEP poly(NIPAAm-co-AAc) as a template for the growth of large (60–150 nm) AuNP have also been carried out.[58] FE-SEM images showed uniform particle sizes as well as contrast effects, showing particle cores with a

TABLE 2 | Polymerization Processes[64–66]

Surfactant-Free Emulsion Polymerization (SFEP) –polymerization initiator soluble in aqueous phase, polymer forms in oil phase –polymerization occurs at oil-water interface	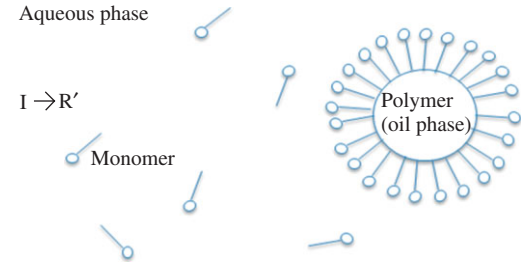
Reverse-Addition Fragmentation Polymerization (RAFT) –requires initiator in presence of chain-transfer agent –living polymerization technique	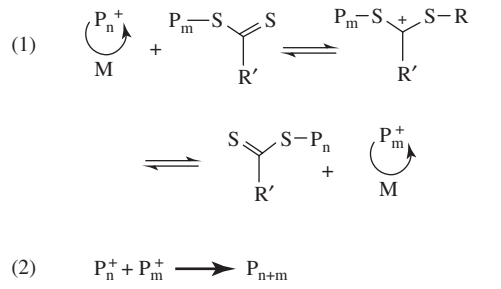
Surface Initiated-Atom Transfer Radical Polymerization (SI-ATRP) –requires a transition metal catalyst, nitrogen-based ligand, and alkyl-halide	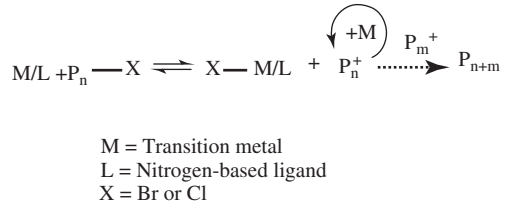

complete hydrogel coating.[26] energy dispersive x-ray spectroscopy (EDX) analysis showed large peaks indicating gold atoms as well as no peaks for the hydrogel polymer, as predicted given the low atomic numbers of the hydrogel elements.[26] Higher resolution transmission electron microscopy (TEM) images show the complete hydrogel shell growth around the particle, as well as differences in hydrogel thickness that could be obtained by minor variations in the monomer and initiator amounts as well as reaction time.[26] However, one drawback of this polymerization method is the encapsulation of multiple particles into one hydrogel matrix.[26] UV–Vis spectroscopy showed minimal changes in the absorption profile of the bare silica–Au nanoshells and hydrogel-coated nanoshells. Dynamic light scattering (DLS) studies show that the hydrodynamic radius of the hydrogel particles decreasing with increasing temperature, an indication of collapse of the hydrogel. The results of this study are summarized in Figure 6.

SI-ATRP Methods

Synthesis of a hydrogel coating using SI-ATRP has also been investigated for its tight control over the thickness of gel produced, providing monodisperse particles. Wei et al. used this method to create a PNIPAAm coating on NIR-absorbing AuNRs.[60] This study used AuNRs with an aspect ratio of 4.4 ± 0.4 and a peak longitudinal plasmon resonance of 843 nm. A disulfide initiator was immobilized onto the AuNR surface followed by *in situ* polymerization of PNIPAAm. TEM characterization of the particles showed that a core/shell structure was formed, and it was noted that the thickness of the coating could be tuned by the polarity of the solvent, with more polar solvents yielding thicker coatings. DLS showed an increase in hydrodynamic diameter at temperatures from 32 to 37°C, indicating the hydrogel coatings had collapsed and become more hydrophobic, causing the particles to precipitate out of solution and aggregate. In addition, a drug-loading experiment with norvancomycin, an antibiotic, showed increased release when the particles were irradiated with an 808 nm laser.

This method has also been employed using iron oxide nanoparticles. Frimpong et al. demonstrated growth of a PNIPAAm hydrogel with poly(ethylene glycol) 400 dimethacrylate (PEG400DMA) cross-links using SI-ATRP on iron oxide particles of 6–10 nm

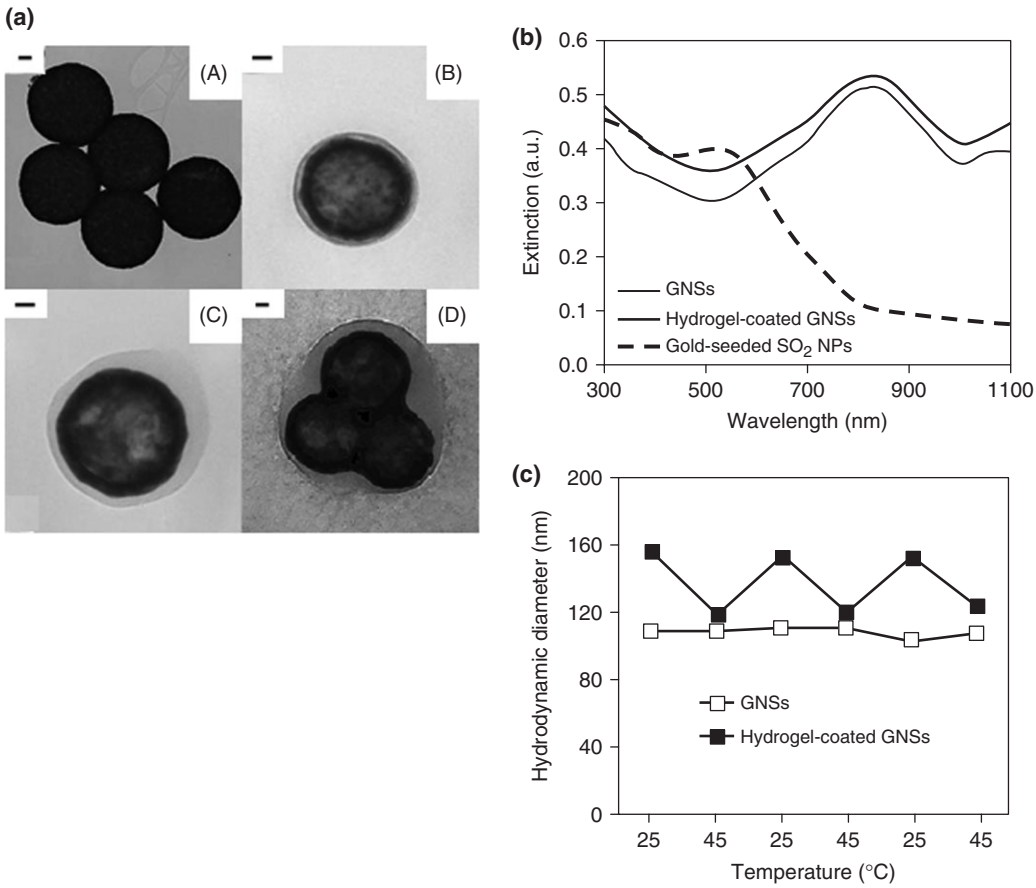

FIGURE 6 | Hydrogel coating by surfactant-free emulsion polymerization (SFEP). (a) TEM images of (A) bare nanoshells (diameter ~120 nm); (B) thin hydrogel-coated nanoshells (diameter ~160 nm); (C) thick hydrogel-coated nanoshells; and (D) multiple encapsulated nanoshells. (b) UV–Vis spectra of gold-seeded silica cores, bare nanoshells, and hydrogel-coated nanoshells. (c) Hydrodynamic diameters of bare nanoshells and hydrogel-coated nanoshells as a function of temperature. (Reprinted with permission from Ref 36. Copyright 2008 Biomedical and Pharmaceutical Engineering Cluster)

diameters.[59] First, the particles were coated with either oleic acid or citric acid followed by a ligand exchange reaction with bromine alkyl halides and a bromosaline to act as initiators of the ATRP reaction of poly(NIPAAm-PEG400DMA). High-resolution TEM analysis showed an ordered crystalline core next to an amorphous polymer shell less than 5 nm thick. DLS analysis showed a larger hydrodynamic diameter of these particles at temperatures from 20 to 30°C with smaller hydrodynamic diameters observed at temperatures above the hydrogel LCST.

Elastin-like Polypeptides

Huang et al. have developed an optically responsive ELP-gold nanorod system.[67] A novel 22-kDa cysteine-containing ELP was conjugated to NIR-absorbing gold nanorods by gold–thiol bonds.[67] The transition temperature (T_t) of the ELP was determined to be 33.4°C; above this temperature the particles aggregated together, resulting in an increase in optical density.[67] NIR irradiation of these particles resulted in an optical response due to a conformational change in the ELP.[67]

CONCLUSION

Researchers have developed thermally responsive polymer–metal nanoparticle composites, showing promise for a wide variety of applications, from drug delivery to microfluidic valve control. These composites can be broken down into three categories: bulk hydrogel systems, microscale systems, and nanoscale coatings. For the field of drug delivery, many 'proof-of-concept' bulk studies have yielded way to studying more nano- and microscale applications. The unique combination of material properties of metal nanoparticles and thermally responsive polymers will undoubtedly have additional applications and will continue to be actively researched in the coming years.

REFERENCES

1. Bromberg LE, Ron ES. Temperature-responsive gels and thermogelling polymer matrices for protein and peptide delivery. *Adv Drug Deliv Rev* 1998, 31:197–221.
2. Qiu Y, Park K. Environment-sensitive hydrogels for drug delivery. *Adv Drug Deliv Rev* 2001, 53:321–339.
3. Chilkoti A, Dreher MR, Meyer DE, Raucher D. Targeted drug delivery by thermally responsive polymers. *Adv Drug Deliv Rev* 2002, 54:613–630.
4. Daniel M-C, Astruc D. Gold nanoparticles: assembly, supramolecular chemistry, quantum-size-related properties, and applications toward biology, catalysis, and nanotechnology. *Chem Rev* 2004, 104:293–346.
5. Averitt RD, Sarkar D, Halas NJ. Plasmon resonance shifts of Au-coated Au_2S nanoshells: insight into multicomponent nanoparticle growth. *Phys Rev Lett* 1997, 78:4217–4220.
6. Hirsch LR, Gobin AM, Lowery AR, Tam F, Drezek RA, Halas NJ, West JL. Metal nanoshells. *Ann Biomed Eng* 2006, 34:15–22.
7. Yu Y-Y, Chang S-S, Lee C-L, Wang CRC. Gold nanorods: electrochemical synthesis and optical properties. *J Phys Chem B* 1997, 101:6661–6664.
8. Gupta AK, Gupta M. Synthesis and surface engineering of iron oxide nanoparticles for biomedical applications. *Biomaterials* 2005, 26:3995–4021.
9. Smith DK, Korgel BA. The importance of the CTAB surfactant on the colloidal seed-mediated synthesis of gold nanorods. *Langmuir* 2008, 24:644–649.
10. Averitt RD, Westcott SL, Halas NJ. Ultrafast optical properties of gold nanoshells. *J Opt Soc Am B* 1999, 16:1814–1823.
11. Weissleder R. A clearer vision for in vivo imaging. *Nat Biotech* 2001, 19:316–317.
12. Turkevich J, Stevenson PC, Hiller J. A study of the nucleation and growth processes in the synthesis of colloidal gold. *Discuss Farad Soc* 1951, 11:55–75.
13. Zhou HS, Honma I, Komlyama H, Haus JW. Controlled synthesis and quantum-size effect in gold-coated nanparticles. *Phys Rev B* 1994, 50:12052–12056.
14. Gobin AM, Watkins EM, Quevedo E, Colvin VL, West JL. Near-infrared-resonant gold/gold sulfide nanoparticles as a photothermal cancer therapeutic agent. *Small* 2010, 6:745–752.
15. Averitt RD, Westcott SL, Halas NJ. Linear optical properties of gold nanoshells. *J Opt Soc Am B* 1999, 16:1824–1832.
16. Loo C, Lowery A, Halas N, West J, Drezek R. Immunotargeted nanoshells for integrated cancer imaging and therapy. *Nano Lett* 2005, 5:709–711.
17. Gobin AM, Lee MH, Halas NJ, James WD, Drezek RA, West JL. Near-infrared resonant nanoshells for combined optical imaging and photothermal cancer therapy. *Nano Lett* 2007, 7:1929–1934.
18. Hirsch LR, Jackson JB, Lee A, Halas NJ, West JL. A whole blood immunoassay using gold nanoshells. *Anal Chem* 2003, 75:2377–2381.
19. Sershen SR, Westcott SL, Halas NJ, West JL. Temperature-sensitive polymer-nanoshell composites for photothermally modulated drug delivery. *J Biomed Mater Res A* 2000, 51:293–298.
20. Sershen SR, Halas NJ, West JL. Pulsatile release of insulin via photothermally modulated drug delivery. *Annu Int Conf IEEE Eng Med Biol Proc* 2002, 1:490–491.
21. Oldenburg SJ, Averitt RD, Westcott SL, Halas NJ. Nanoengineering of optical resonances. *Chem Phys Lett* 1998, 288:243–247.
22. Sershen SR, Westcott SL, West JL, Halas NJ. An opto-mechanical nanoshell-polymer composite. *Appl Phys B* 2001, 73:379–381.
23. Sershen SR, Ng M, Halas NJ, West JL. Optically controllable materials: potential valves and actuators in microfluidics and MEMs. *Annu Int Conf IEEE Eng Med Biol Proc* 2002, 3:1822–1823.
24. Sershen SR, Mensing GA, Ng M, Halas NJ, Beebe DJ, West JL. Independent optical control of microfluidic valves formed from optomechnically responsive nanocomposite hydrogels. *Adv Mater* 2005, 17:1366–1368.
25. Bikram M, Gobin AM, Whitmire RE, West JL. Temperature-sensitive hydrogels with SiO2-Au nanoshells for controlled drug delivery. *J Control Release* 2007, 123:219–227.
26. Kim J-H, Lee TR. Thermo-responsive hydrogel-coated nanoshells for in vivo drug delivery. *J Biomed Pharm Eng* 2008, 2:29–35.
27. Mohamed MB, Ismail KZ, Link S, El-Sayed MA. Thermal reshaping of gold nanorods in micelles. *J Phys Chem B* 1998, 102:9370–9374.
28. Nikoobakht B, El-Sayed MA. Preparation and growth mechanism of gold nanorods (NRs) using seed-mediated growth method. *Chem Mater* 2003, 15:1957–1962.
29. Galaev IY, Mattiasson B. 'Smart' polymers and what they could do in biotechnology and medicine. *Trends Biotechnol* 1999, 17:335–340.
30. Bikram M, West JL. Thermo-responsive systems for controlled drug delivery. *Expert Opin Drug Deliv* 2008, 5:1077–1091.
31. Meyer DE, Shin BC, Kong GA, Dewhirst MW, Chilkoti A. Drug targeting using thermally responsive

polymers and local hyperthermia. *J Control Release* 2001, 74:213–224.

32. Schild HG. Poly(N-isopropylacrylamide): experiment, theory and application. *Prog Polym Sci* 1992, 17: 163–249.
33. Sasaki S, Kawasaki H, Maeda H. Volume phase transition behavior of N-isopropylacrylamide gels as a function of the chemical potential of water molecules. *Macromolecules* 1996, 30:1847–1848.
34. Yoshida R, Sakai K, Okano T, Sakurai Y. Modulating the phase transition temperature and thermosensitivity in N-isopropylacrylamide copolymer gels. *J Biomater Sci Polym Ed* 1994, 6:585–598.
35. Keerl M, Smirnovas V, Winter R, Richtering W. Copolymer microgels from mono- and disubstituted acrylamides: phase behavior and hydrogen bonds. *Macromolecules* 2008, 41:6830–6836.
36. Owens DE, Eby JK, Jian Y, Peppas NA. Temperature-responsive polymer-gold nanocomposites as intelligent therapeutic systems. *J Biomed Mater Res A* 2007, 83A:692–695.
37. Owens DE, Jian Y, Fang JE, Slaughter BV, Chen Y-H, Peppas NA. Thermally responsive swelling properties of polyacrylamide/poly(acrylic acid) interpenetrating polymer network nanoparticles. *Macromolecules* 2007, 40:7306–7310.
38. Urry DW. Physical chemistry of biological free energy transduction as demonstrated by elastic protein-based polymers. *J Phys Chem B* 1997, 101:11007–11028.
39. Satarkar NS, Zach Hilt J. Magnetic hydrogel nanocomposites for remote controlled pulsatile drug release. *J Control Release* 2008, 130:246–251.
40. Satarkar NS, Zhang W, Eitel RE, Zach Hilt J. Magnetic hydrogel nanocomposites as remote controlled microfluidic valves. *Lab Chip* 2009, 9:1773–1779.
41. Kim J, Serpe MJ, Lyon LA. Photoswitchable microlens arrays. *Angew Chem Int Ed* 2005, 44:1333–1336.
42. Wang C, Flynn NT, Langer R. Controlled structure and properties of thermoresponsive nanoparticle-hydrogel composites. *Adv Mater* 2004, 16:1074–1079.
43. Wang C, Flynn NT, Langer R. Morphologically well-defined gold nanoparticles embedded in thermo-responisve hydrogel matrices. In: *Materials Research Society Symposium Proceedings*, Materials Research Society, Warrendale, PA; Vol. 820; 2004, 333–338.
44. Frimpong RA, Fraser S, Zach Hilt J. Synthesis and temperature response analysis of magnetic-hydrogel nanocomposites. *J Biomed Mater Res A* 2007, 80A:1–6.
45. Satarkar NS, Zach Hilt J. Hydrogel nanocomposites as remote-controlled biomaterials. *Acta Biomater* 2008, 4:11–16.
46. Meenach SA, Anderson AA, Suthar M, Anderson KW, Zach Hilt J. Biocompatibility analysis of magnetic hydrogel nanocomposites based on poly(N-isopropylacrylamide) and iron oxide. *J Biomed Mater Res A* 2009, 91:903–909.
47. Katchalsky A, Eisenberg H, Lifson S. Hydrogen bonding and ionization of carboxylic acids in aqueous solutions. *J Am Chem Soc* 1951, 73:5889–5890.
48. Zhao X, Ding X, Deng Z, Zheng Z, Peng Y, Long X. Thermoswitchable electronic properties of a gold nanoparticle/hydrogel composite. *Macromol Rapid Commun* 2005, 26:1784–1787.
49. Zhao X, Ding X, Deng Z, Zheng Z, Peng Y, Tian C, Long X. A kind of smart gold nanoparticle–hydrogel composite with tunable thermo-switchable electrical properties. *New J Chem* 2006, 30:915–920.
50. Li J, He W-D, Sun X-L. Preperation of poly(styrene-b-N-isopropylacyrlamide) micelles surface-linked with gold nanoparticles and thermo-responsive ultra-violet-visible absorbance. *J Polym Sci A Polym Chem* 2007, 45:5156–5163.
51. Kim D-H, Rozhkova EA, Rajh T, Bader SD, Novosad V. Synthesis of hybrid gold/iron oxide nanoparticles in block copolymer micelles for imaging, drug delivery, and magnetic hyperthermia. *IEEE Trans Magn* 2009, 45:4821–4824.
52. Hoare T, Santamaria J, Goya GF, Irusta S, Lin D, Lau S, Padera R, Langer R, Kohane DS. A magnetically triggered composite membrane for on-demand drug delivery. *Nano Lett* 2009, 9:3651–3657.
53. Shan J, Chen J, Nuopponen M, Tenhu H. Two phase transitions of poly(N-isopropylacrylamide) brushes bound to gold nanoparticles. *Langmuir* 2004, 20:4671–4676.
54. Shan J, Nuopponen M, Jiang H, Viitala T, Kauppinen E, Kontturi K, Tenhu H. Amphiphilic gold nanoparticles grafted with poly(N-isopropylacrylamide) and polystyrene. *Macromolecules* 2005, 38:2918–2926.
55. Nupponen M, Tenhu H. Gold nanoparticles protected with ph and temperature-sensitive diblock copolymers. *Langmuir* 2007, 23:5352–5357.
56. Yusa S-I, Fukuda K, Yamamoto T, Iwasaki Y, Watanabe A, Akiyoshi K, Morishima Y. Salt effect on the heat-induced association behavior of gold nanoparticles coated with poly(N-isopropylacrylamide) prepared via reversible addition-fragmentation chain transfer (RAFT) radical polymerization. *Langmuir* 2007, 23:12842–12848.
57. Kim J-H, Lee TR. Discrete thermally responsive hydrogel-coated gold nanoparticles for use as drug-delivery vehicles. *Drug Dev Res* 2006, 67:61–69.
58. Kim J-H, Lee TR. Hydrogel-templated growth of large gold nanoparticles: synthesis of thermally responsive hydrogel–nanoparticle composites. *Langmuir* 2007, 23:6504–6509.

59. Frimpong RA, Zach Hilt J. Poly(N-isopropylacrylamide)-based hydrogel coatings on magnetite nanoparticles via atom transfer radical polymerization. *Nanotechnology* 2008, 19:175101.
60. Wei Q, Ji J, Shen J. Synthesis of near-infrared responsive gold nanorod/PNIPAAm core/shell nanohybrids via surface initiated ATRP for smart drug delivery. *Macromol Rapid Commun* 2008, 29:645–650.
61. Chakraborty S, Bishnoi SW, Perez-Luna VH. Gold nanoparticles with poly(N-isopropylacrylamide) formed via surface initiated atom transfer free radical polymerization exhibit unusually slow aggregation kinetics. *J Phys Chem C* 2010, 114:5947–5955.
62. Singh N, Lyon LA. Au nanoparticle templated synthesis of pNIPAm nanogels. *Chem Mater* 2007, 19:719–726.
63. Morones JR, Frey W. Room temperature synthesis of an optically and thermally responsive hybrid PNIPAM-gold nanoparticle. *J Nanoparticle Res* 2009, 12:1401–1414.
64. Odian GG. *Principles of Polymerization*. Hoboken, NJ: Wiley-Interscience; 2004.
65. Barner-Kowollik C, Quinn JF, Morsley DR, Davis TP. Modeling the reversible addition–fragmentation chain transfer process in cumyl dithiobenzoate-mediated styrene homopolymerizations: assessing rate coefficients for the addition–fragmentation equilibrium. *J Polym Sci A Polym Chem* 2001, 39:1353–1365.
66. Xu FJ, Neoh KG, Kang ET. Bioactive surfaces and biomaterials via atom transfer radical polymerization. *Prog Polym Sci* 2009, 34:719–761.
67. Huang HC, Koria P, Parker SM, Selby L, Megeed Z, Rege K. Optically responsive gold nanorod–polypeptide assemblies. *Langmuir* 2008, 24:14139–14144.

